

Response to referee comments

We thank the referee for their thorough review and helpful suggestions. The reviewer's comments (in black) and our responses follow.

The manuscript provides a thorough diagnosis of Hg chemical processing in the lower, middle, and upper troposphere within the GEOS-Chem model. The results are an incremental advance over past work in establishing the important role of oxidation in the middle and upper troposphere. The main advance over past work is in diagnosing the subtropical anticyclones as conduits for Hg(II) to the lower troposphere.

I concur with the other reviewer who commented on the lack of model comparisons to aircraft data and observations in the subtropics, since that is where much of the action in the model is happening. The authors' earlier work with aircraft could be included in discussion (Shah et al., 2016). It would also be very helpful to compare the model to surface observations in the subtropics, where they are available (e.g. Sheu et al., 2010).

We have significantly expanded our model-observation comparison to include 14 additional stations measuring Hg wet deposition, 14 additional stations measuring Hg(II) surface concentrations, some of which are in the subtropics, and two-aircraft based campaigns where Hg(II) was measured (the campaign over Tullahoma, TN and NOMADSS). Tables S1 and S2, and Figs. S1, S2 and S3 at the end of the document will be included in the supplement to the manuscript.

Likewise, I agree with the reviewer who pointed out that simulations for 2013-2014 are compared with AMNet observations for 2009-2012 without discussion of interannual variability.

Good point. From the 4-year (2013-16) "dry-Hg(II)" simulation, we find that the variation in the modeled 2-year average Hg(II) concentrations at the AMNet sites vary by $\pm 30\%$.

We have added the following to Sect 2.3.3 "Comparing observations and simulations for different time periods adds additional uncertainty due to inter-annual variations. From four years of model simulation (2013-16), we estimate this uncertainty at $\pm 30\%$."

The title is too sweeping. It implies that Hg(II) emissions and Hg(II) produced in the lower troposphere are minor sources of Hg(II) deposition. While that may be true on a global average basis (Table 1), Figure 5 shows that Hg(II) emissions contribute more than 50% of deposition in major industrial regions and lower troposphere Hg(II) dominates in polar regions. The 2x2.5 degree resolution of the model also likely dilutes the importance of Hg(II) emissions near large sources. These caveats are critical for policymakers, but are not reflected in the title or mentioned in the abstract.

Excellent point. We have revised the title such that the importance of emissions and production in the lower troposphere is not diminished, and the role of the subtropics is highlighted. The new title is: "Subtropical subsidence and surface deposition of oxidized mercury produced in the free troposphere."

We have also clarified the limitations of the coarse resolution of the global model by adding to the abstract the following (underlined text added):

"...whereas 26–66% of surface Hg(II) over the eastern U.S., Europe, East Asia, and South Asia is directly emitted. The influence of directly emitted Hg(II) near emissions sources is likely higher, but cannot be quantified by our coarse-resolution global model(2° latitude $\times 2.5^\circ$ longitude). Over the oceans..."

In Sect. 3.2 we have added the underlined text:

"We calculate that 27–69% of surface Hg(II) in eastern U.S., Europe, East and South Asia consists of E-Hg(II) (Fig. 6b). The contribution of E-Hg(II) is 80% of higher in areas close to

emission sources (Fig. 5e), and can be even higher within tens of kilometers of the sources. However, the near-source contribution of emitted Hg(II) cannot be estimated with our 2° latitude $\times 2.5^\circ$ longitude global model.”

And, in the conclusion, we have added the following underlined text:

“...the wet deposition flux in these regions is largely (~90%) the result of Hg(II) produced in the upper and middle troposphere. The contribution of directly emitted Hg(II) can be higher within tens of kilometers of a source, but cannot be quantified by our coarse-resolution global model.”

My remaining comments are minor.

Please specify the version of the GEOS-Chem model used in this work.

It is v9-02.

We have made the following change to Sect. 2.2: “...resolution of 2° latitude $\times 2.5^\circ$ longitude and 47 vertical levels for the GEOS-Chem simulations in this study. We use GEOS-Chem v9-02 (<http://acmg.seas.harvard.edu/geos/>). Global anthropogenic emissions...”

Eq. R1 has a typo “15” in it.

Fixed the typo.

The rate coefficient k_{lf} appears to be missing an exponent. Please check all rate expressions

Fixed the error and double-checked the rate expressions. They now are as follows:

$$k_{lf} = 1.46 \times 10^{-32} \times \left(\frac{T}{298}\right)^{-1.86} \times [M] \text{ cm}^3 \text{ molecule}^{-1} \text{ s}^{-1}$$

$$k_{lr} = 2.67 \times 10^{41} \times \exp\left(\frac{-7292}{T}\right) \times \left(\frac{T}{298}\right)^{1.76} \times k_{lf} \text{ s}^{-1}$$

$$k_2 = 3.9 \times 10^{-11} \text{ cm}^3 \text{ molecule}^{-1} \text{ s}^{-1}$$

$$k_3 = 2.5 \times 10^{-10} \times \left(\frac{T}{298}\right)^{-0.57} \text{ cm}^3 \text{ molecule}^{-1} \text{ s}^{-1}$$

P11, L1: typo: “tmodeled”

Fixed the typo.

Table 1 and P12 report a 45 day lifetime for STRAT Hg(II). That seems surprisingly short considering that nearly zero reduction should happen in the stratosphere, based on the model assumption that reduction requires liquid water clouds. Based on context, I think the authors mean that the lifetime of Hg(II) produced in the stratosphere is 45 days once it enters the troposphere, but this is not clear.

That is right. The lifetime is for the STRAT Hg(II) present in the troposphere.

On P12 we have clarified this as follows: “As summarized in Table 1, we find that the tropospheric lifetime of Hg(II)...” (underlined text added). We have changed the last row of Table 1 to: “Hg(II) tropospheric lifetime [days]”

Section 5 addresses the contribution of upper tropospheric Hg(II) to surface deposition across the US. Other recent papers on this topic are Weiss-Penzias et al., (2015); Shanley et al., (2015); Coburn et al., (2016); Kaulfus et al., (2017).

We have now added citations to these papers in the manuscript.

P18L6. The regression equation is not adequately explained. The units of each variable and coefficient must be provided. Is the regression equation fitted to the observed or modeled Hg fluxes?

The regression equation is now clarified, with units for the variables and the coefficients. It is fitted to the observed fluxes.

Table S1: List of stations with observations of Hg wet deposition used in this study

Site ID	Site Name	Latitude	Longitude	Elevation (m.a.s.l.)	Measurement period	Network/ Region
CO96	Molas Pass	37.75	-107.69	3248	2013-2014	MDN ^a
FL11	Everglades National Park-Research Center	25.39	-80.68	2	2013-2014	MDN
WA18	Seattle/NOAA	47.68	-122.26	11	2013-2014	MDN
TX21	Longview	32.38	-94.71	103	2013-2014	MDN
VT99	Underhill	44.53	-72.87	399	2013-2014	MDN
VA28	Shenandoah National Park-Big Meadows	38.52	-78.43	1072	2013-2014	MDN
WI36	Trout Lake	46.05	-89.65	509	2013-2014	MDN
WI99	Lake Geneva	42.58	-88.50	288	2013-2014	MDN
PA29	Kane Experimental Forest	41.60	-78.77	618	2013-2014	MDN
PA42	Leading Ridge	40.66	-77.94	287	2013-2014	MDN
PA72	Milford	41.33	-74.82	212	2013-2014	MDN
TN11	Great Smoky Mountains	35.66	-83.59	640	2013-2014	MDN
MN18	Fernberg	47.95	-91.50	524	2013-2014	MDN
ME02	Bridgton	44.11	-70.73	222	2013-2014	MDN
ME96	Casco Bay-Wolfe's Neck Farm	43.83	-70.06	15	2013-2014	MDN
NC08	Waccamaw State Park	34.26	-78.48	10	2013-2014	MDN
PA13	Allegheny Portage Historic Site	40.46	-78.56	739	2013-2014	MDN
PA90	Hills Creek State Park	41.80	-77.19	476	2013-2014	MDN
SC19	Congaree Swamp	33.81	-80.78	34	2013-2014	MDN
IL11	Bondville	40.05	-88.37	212	2013-2014	MDN
FL34	Everglades Nutrient Removal Project	26.66	-80.40	10	2013-2014	MDN
FL05	Chassahowitzka National Wildlife Refuge	28.75	-82.56	3	2013-2014	MDN
GA09	Okefenokee National Wildlife Refuge	30.74	-82.13	45	2013-2014	MDN
PA00	Arendtsville	39.92	-77.31	269	2013-2014	MDN
KS32	Lake Scott State Park	38.67	-100.92	863	2013-2014	MDN
ME98	Acadia National Park-McFarland Hill	44.38	-68.26	150	2013-2014	MDN
ME00	Caribou	46.87	-68.01	191	2013-2014	MDN
ME09	Greenville Station	45.49	-69.66	322	2013-2014	MDN
MN16	Marcell Experimental Forest	47.53	-93.47	431	2013-2014	MDN
MN23	Camp Ripley	46.25	-94.50	410	2013-2014	MDN
MN27	Lamberton	44.24	-95.30	367	2013-2014	MDN
MO03	Ashland Wildlife Area	38.75	-92.20	257	2013-2014	MDN
MT05	Glacier National Park-Fire Weather Station	48.51	-114.00	964	2013-2014	MDN
NE15	Mead	41.15	-96.49	352	2013-2014	MDN
NY20	Huntington Wildlife	43.97	-74.22	500	2013-2014	MDN
NY68	Biscuit Brook	41.99	-74.50	634	2013-2014	MDN
PA37	Waynesburg	39.82	-80.29	452	2013-2014	MDN
MI48	Seney National Wildlife Refuge-Headquarters	46.29	-85.95	220	2013-2014	MDN
SC05	Cape Romain National Wildlife Refuge	32.94	-79.66	1	2013-2014	MDN
SC03	Savannah River	33.25	-81.65	90	2013-2014	MDN
PA60	Valley Forge	40.12	-75.88	46	2013-2014	MDN
PA30	Erie	42.16	-80.11	177	2013-2014	MDN

Table S1 continued

Site ID	Site Name	Latitude	Longitude	Elevation	Measurement	Network/
AL03	Centreville	32.90	-87.25	135	2013-2014	MDN
GA40	Yorkville	33.93	-85.05	395	2013-2014	MDN
MO46	Mingo National Wildlife Refuge	36.97	-90.14	105	2013-2014	MDN
KY10	Mammoth Cave National Park	37.13	-86.15	236	2013-2014	MDN
MS22	Oak Grove	30.98	-88.93	100	2013-2014	MDN
WI31	Devil's Lake	43.44	-89.68	389	2013-2014	MDN
PA47	Millersville	39.99	-76.39	84	2013-2014	MDN
GA33	Sapelo Island	31.40	-81.28	3	2013-2014	MDN
OK99	Stilwell	35.75	-94.67	299	2013-2014	MDN
NV02	Lesperance Ranch	41.50	-117.50	1388	2013-2014	MDN
MD99	Beltsville	39.03	-76.82	46	2013-2014	MDN
MD08	Piney Reservoir	39.71	-79.01	769	2013-2014	MDN
NJ30	New Brunswick	40.47	-74.42	21	2013-2014	MDN
ON07	Egbert	44.23	-79.79	196	2013-2014	MDN
WI10	Potawatomi	45.56	-88.81	570	2013-2014	MDN
WA03	Makah National Fish Hatchery	48.29	-124.65	6	2013-2014	MDN
CA94	Converse Flats	34.19	-116.91	1724	2013-2014	MDN
CA20	Yurok Tribe-Requa	41.56	-124.09	110	2013-2014	MDN
OK01	McGee Creek	34.32	-95.89	195	2013-2014	MDN
OK31	Copan	36.91	-95.88	255	2013-2014	MDN
SD18	Eagle Butte	44.99	-101.24	742	2013-2014	MDN
MD00	Smithsonian Environmental Research Center	38.89	-76.56	20	2013-2014	MDN
FL97	Everglades-Western Broward County	26.17	-80.82	4	2013-2014	MDN
UT97	Salt Lake City	40.71	-111.96	1297	2013-2014	MDN
OK04	Lake Murray	34.10	-97.07	245	2013-2014	MDN
PA52	Little Pine State Park	41.36	-77.36	228	2013-2014	MDN
KS03	Reserve	39.98	-95.57	265	2013-2014	MDN
KS24	Glen Elder State Park	39.51	-98.34	456	2013-2014	MDN
KS99	Cimarron National Grassland	37.13	-101.82	1021	2013-2014	MDN
OK06	Wichita Mountains	34.73	-98.71	492	2013-2014	MDN
KS04	West Mineral	37.27	-94.94	274	2013-2014	MDN
NY43	Rochester	43.15	-77.55	136	2013-2014	MDN
NY06	Bronx	40.87	-73.88	68	2013-2014	MDN
MN98	Blaine	45.14	-93.22	275	2013-2014	MDN
MS12	Grand Bay NERR	30.43	-88.43	2	2013-2014	MDN
PA21	Goddard State Park	41.43	-80.15	385	2013-2014	MDN
FL96	Pensacola	30.55	-87.38	45	2013-2014	MDN
AL19	Birmingham	33.55	-86.81	200	2013-2014	MDN
DE0008R	Schmücke	50.65	10.77	937	2013-2014	EMEP ^b
FI0036R	Pallas (Matorova)	68.00	24.24	340	2013-2014	EMEP
GB0036R	Harwell	51.57	-1.32	137	2013-2014	EMEP
GB0048R	Auchencorth Moss	55.79	-3.24	260	2013-2014	EMEP
NO0001R	Birkenes	58.38	8.25	190	2013-2014	EMEP
SE0005R	Bredkälen	63.85	15.33	404	2013-2014	EMEP
SE0011R	Vavihill	56.02	13.15	175	2013-2014	EMEP
SE0014R	Råö	57.39	11.91	5	2013-2014	EMEP
NYA	Ny-Ålesund	78.90	11.88	12	2013-2014	GMOS ^c
MHE	Mace Head	53.33	-9.91	5	2013	GMOS
ISK	Iskrba	45.56	14.86	520	2013-2014	GMOS
SIS	Sisal	21.16	-90.05	7	2013-2014	GMOS
AMS	Amsterdam Island	-37.80	77.55	3	2013-2014	GMOS

Table S1 continued

Site ID	Site Name	Latitude	Longitude	Elevation	Measurement	Network/
CGR	Cape Grim	-40.68	144.69	94	2013-2014	GMOS
MCB	Mt. Changbai	42.41	128.11	736	2011-2014	China ^d
MDM	Mt. Damei	29.63	121.57	550	2012-2014	China
MLG	Mt. Leigong	26.39	108.20	2176	2008-2009	China
MAL	Mt. Ailao	24.53	101.11	2450	2011-2014	China
MWA	Mt. Waliguan	36.29	100.90	3816	2012-2014	China
BYB	Bayinbuluk	42.89	83.72	2500	2013-2014	China
PEN	Pengjiayu	25.63	122.07	102	2009	Taiwan ^e
PR20	El Verde	18.32	-65.82	380	2015	MDN

(a) <http://nadp.sws.uiuc.edu/mdn/>(b) <http://www.nilu.no/projects/ccc/index.html>

(c) Sprovieri et al. (2017)

(d) Fu et al. (2016)

(e) Sheu and Lin (2013)

Table S2: List of ground stations with observations of Hg(II) surface concentrations used in this study

Site ID	Site Name	Latitude	Longitude	Elevation (m.a.s.l.)	Measurement period	Network/ Region
AL19	Birmingham	33.55	-86.81	177	2009-2012	AMNet ^a
CA48	Elkhorn Slough	36.81	-121.78	10	2010-2011	AMNet
FL96	Pensacola	30.55	-87.38	44	2009-2012	AMNet
GA40	Yorkville	33.93	-85.05	394	2009-2012	AMNet
MD08	Piney Reservoir	39.71	-79.01	761	2009-2012	AMNet
MD96	Beltsville_B	39.03	-76.82	47	2009-2012	AMNet
MD97	Beltsville	39.03	-76.82	47	2009-2012	AMNet
MS12	Grand Bay NERR	30.41	-88.40	1	2009-2012	AMNet
MS99	Grand Bay NERR_B	30.41	-88.40	1	2009-2012	AMNet
NH06	Thompson Farm	43.11	-70.95	25	2009-2011	AMNet
NJ05	Brigantine	39.46	-74.45	8	2009-2012	AMNet
NS01	Kejimkujik	44.43	-65.20	158	2009-2012	AMNet
NY06	New York City	40.87	-73.88	26	2009-2012	AMNet
NY20	Huntington Wildlife Forest	43.97	-74.22	502	2009-2012	AMNet
NY43	Rochester	43.15	-77.62	154	2009	AMNet
NY95	Rochester_B	43.15	-77.55	154	2009-2012	AMNet
OH02	Athens	39.31	-82.12	274	2009-2012	AMNet
OK99	Stilwell	35.75	-94.67	300	2009-2012	AMNet
PA13	Allegheny Portage	40.46	-78.56	739	2009-2012	AMNet
UT96	Antelope Island	41.09	-112.12	1285	2009-2011	AMNet
UT97	Salt Lake City	40.71	-111.96	1099	2009-2012	AMNet
VT99	Underhill	44.53	-72.87	397	2009-2012	AMNet
WI07	Horicon	43.46	-88.62	272	2009-2012	AMNet
WV99	Canaan Valley Institute	39.12	-79.45	985	2009-2012	AMNet
AMS	Amsterdam Island	-37.80	77.55	70	2012-13	GMOS ^b
RAO	Råö	57.39	11.91	7	2012-15	GMOS ^c
LON	Longobucco	39.39	16.61	1379	2013	GMOS ^d
MAN	Manaus	-2.89	-59.97	110	2013	GMOS ^d
WAL	Waldhof	52.80	10.76	74	2009-2011	Germany ^e
MCH	Mt. Changbai	42.40	128.11	740	2013-2014	China ^f
MWA	Mt. Waliguan	36.29	100.90	3816	2007-2008	China
MAL	Mt. Ailao	24.53	101.02	2450	2011-2012	China
SLA	Shangri-La	28.02	99.73	3580	2009-2010	China
MYU	Miyun	40.48	116.76	220	2008-2009	China
MDA	Mt. Damei	29.63	121.57	550	2011-2013	China
MGO	Mt. Gongga	29.65	102.12	1640	2005-2007	China
LABS	Lulin Atmospheric Background Station	23.51	120.92	2862	2006-2007	Taiwan ^g
ALE	Alert	82.49	-62.34	210	2009-2011	Canada ^h

(a) <http://nadp.sws.uiuc.edu/amn/>

(b) Angot et al. (2014)

(c) Wängberg et al. (2016)

(d) Travnikov et al. (2017)

(e) Weigelt et al. (2013)

(f) Fu et al. (2015)

(g) Sheu et al. (2010)

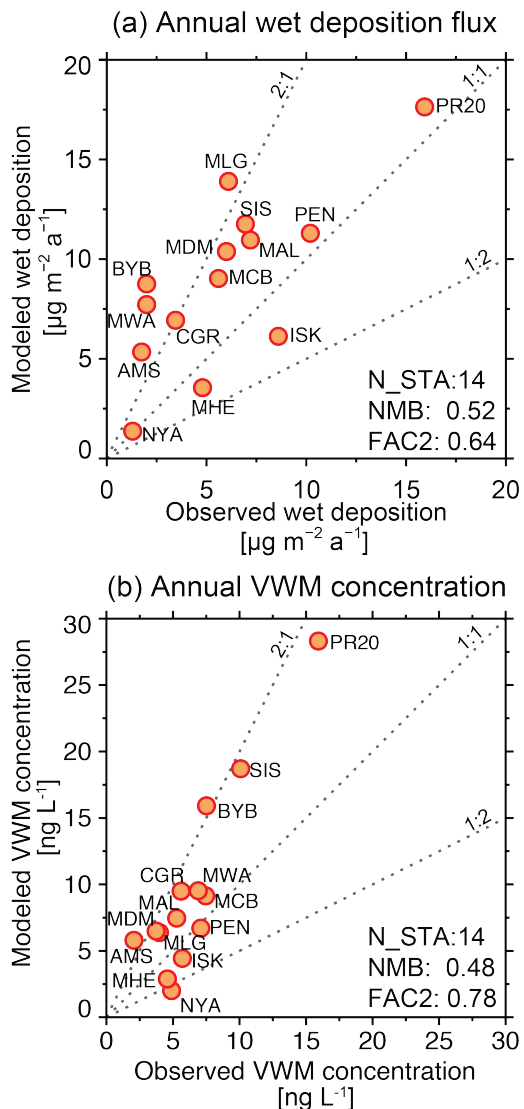


Figure S1 (a) Simulated and observed Hg wet deposition flux for GMOS and other stations listed in Table S1. (b) Simulated and observed annual volume-weighted mean (VWM) Hg concentration for GMOS and other stations listed in Table S1. The number of stations (N_STA), normalized mean bias (NMB; $\text{NMB} = \sum_i (M_i - O_i) / \sum_i O_i \times 100\%$), and FAC2 (percentage of points where $0.5 \leq M_i/O_i \leq 2$ where O_i and M_i are observed and simulated values, respectively) is included in both panels.

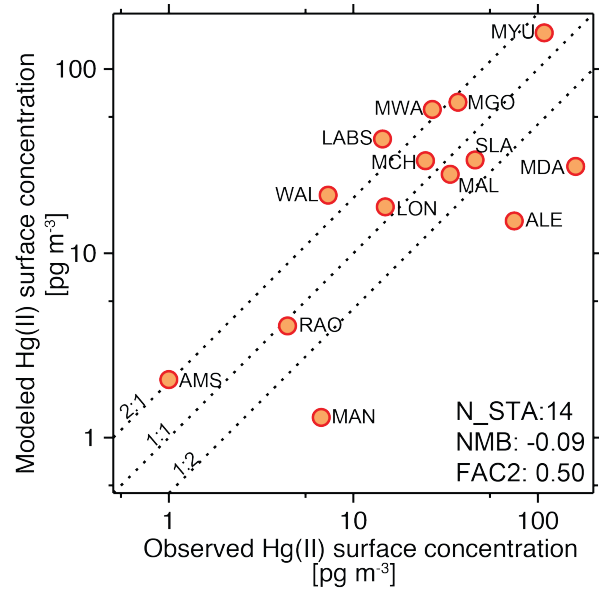


Figure S2 Simulated and observed surface Hg(II) concentration for GMOS and other stations listed in Table S1.
Note the logarithmic scale on both axes.

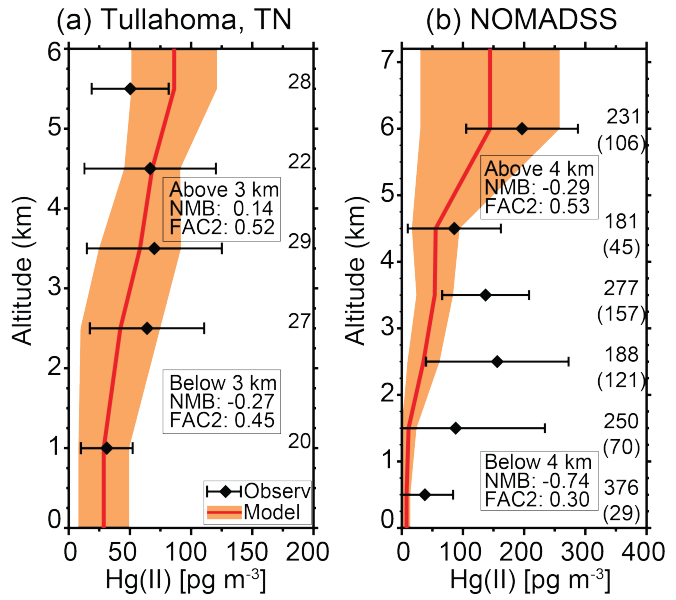


Figure S3 (a) Simulated and observed Hg(II) concentrations for aircraft-based campaign over Tullahoma, TN, USA (2012-2013) (Brooks et al., 2013). (b) Simulated and observed Hg(II) concentrations for the NOMADSS aircraft-based campaign (2013) (Shah et al., 2016). The number of model-observation pairs in each height bin is shown in panel (a). In panel (b), the number of model-observation pairs in each height bin, and, in parentheses, the number of model-observation pairs where the observations were above the instrument detection limit, are shown.

REFERENCES

- Angot, H., Barret, M., Magand, O., Ramonet, M. and Dommergue, A.: A 2-year record of atmospheric mercury species at a background Southern Hemisphere station on Amsterdam Island, *Atmospheric Chem. Phys.*, 14(20), 11461–11473, doi:10.5194/acp-14-11461-2014, 2014.
- Brooks, S., Ren, X., Cohen, M., Luke, W. T., Kelley, P., Artz, R., Hynes, A., Landing, W. and Martos, B.: Airborne Vertical Profiling of Mercury Speciation near Tullahoma, TN, USA, *Atmosphere*, 5(3), 557, doi:10.3390/atmos5030557, 2014.
- Coburn, S., Dix, B., Edgerton, E., Holmes, C. D., Kinnison, D., Liang, Q., Schure, ter, A., Wang, S. and Volkamer, R.: Mercury oxidation from bromine chemistry in the free troposphere over the southeastern US, *Atmos. Chem. Phys.*, 16(6), 3743–3760, doi:10.5194/acp-16-3743-2016, 2016.
- Fu, X., Yang, X., Lang, X., Zhou, J., Zhang, H., Yu, B., Yan, H., Lin, C.-J. and Feng, X.: Atmospheric wet and litterfall mercury deposition at urban and rural sites in China, *Atmospheric Chem. Phys.*, 16(18), 11547–11562, doi:10.5194/acp-16-11547-2016, 2016.
- Fu, X. W., Zhang, H., Yu, B., Wang, X., Lin, C.-J. and Feng, X. B.: Observations of atmospheric mercury in China: a critical review, *Atmospheric Chem. Phys.*, 15(16), 9455–9476, doi:10.5194/acp-15-9455-2015, 2015.
- Kaulfus, A. S., Nair, U., Holmes, C. D. and Landing, W. M.: Mercury Wet Scavenging and Deposition Differences by Precipitation Type, *Environ. Sci. Technol.*, 51(5), 2628– 2634, doi:10.1021/acs.est.6b04187, 2017.
- Shah, V., Jaeglé, L., Gratz, L. E., Ambrose, J. L., Jaffe, D. A., Selin, N. E., Song, S., Campos, T. L., Flocke, F. M., Reeves, M., Stechman, D., Stell, M., Festa, J., Stutz, J., Weinheimer, A. J., Knapp, D. J., Montzka, D. D., Tyndall, G. S., Apel, E. C., Hornbrook, R. S., Hills, A. J., Riemer, D. D., Blake, N. J., Cantrell, C. A. and Mauldin III, R. L.: Origin of oxidized mercury in the summertime free troposphere over the southeastern US, *Atmospheric Chem. Phys.*, 16(3), 1511–1530, doi:10.5194/acp-16-1511-2016, 2016.
- Shanley, J. B.; Engle, M. a.; Scholl, M.; Krabbenhoft, D. P.; Brunette, R.; Olson, M. L.; Conroy, M. E. High Mercury Wet Deposition at a "clean Air" Site in Puerto Rico. *Environ. Sci. Technol.* 2015, 49, 12474–12482.
- Sheu, G.-R. and Lin, N.-H.: Characterizations of wet mercury deposition to a remote islet (Pengjiayu) in the subtropical Northwest Pacific Ocean, *Atmos. Environ.*, 77, 474–481, doi:10.1016/j.atmosenv.2013.05.038, 2013.
- Sheu, G.-R., Lin, N.-H., Wang, J.-L., Lee, C.-T., Yang, C.-F. O. and Wang, S.-H.: Temporal distribution and potential sources of atmospheric mercury measured at a high-elevation background station in Taiwan, *Atmos. Environ.*, 44(20), 2393–2400, doi:10.1016/j.atmosenv.2010.04.009, 2010.
- Sprovieri, F., Pirrone, N., Bencardino, M., D'Amore, F., Angot, H., Barbante, C., Brunke, E.-G., Arcega-Cabrera, F., Cairns, W., Comero, S., Diéguez, M. D. C., Dommergue, A., Ebinghaus, R., Feng, X. B., Fu, X., Garcia, P. E., Gawlik, B. M., Hageström, U., Hansson, K., Horvat, M., Kotnik, J., Labuschagne, C., Magand, O., Martin, L., Mashyanov, N., Mkololo, T., Munthe, J., Obolkin, V., Ramirez Islas, M., Sena, F., Somerset, V., Spandow, P., Vardè, M., Walters, C., Wängberg, I., Weigelt, A., Yang, X. and Zhang, H.: Five-year records of mercury wet deposition flux at GMOS sites in the Northern and Southern hemispheres, *Atmospheric Chem. Phys.*, 17(4), 2689–2708, doi:10.5194/acp-17-2689-2017, 2017.
- Travnikov, O., Angot, H., Artaxo, P., Bencardino, M., Bieser, J., D'Amore, F., Dastoor, A., De Simone, F., Diéguez, M. D. C., Dommergue, A., Ebinghaus, R., Feng, X. B., Gencarelli, C. N., Hedgecock, I. M., Magand, O., Martin, L., Matthias, V., Mashyanov, N., Pirrone, N., Ramachandran, R., Read, K. A., Ryjkov, A., Selin, N. E., Sena, F., Song, S., Sprovieri, F., Wip, D., Wängberg, I. and Yang, X.: Multi-model study of mercury dispersion in the atmosphere: atmospheric processes and model evaluation, *Atmospheric Chem. Phys.*, 17(8), 5271–5295, doi:10.5194/acp-17-5271-2017, 2017.
- Wängberg, I., Nerentorp Mastromonaco, M. G., Munthe, J. and Gårdfeldt, K.: Airborne mercury species at the Råö background monitoring site in Sweden: distribution of mercury as an effect of long-range transport, *Atmospheric Chem. Phys.*, 16(21), 13379–13387, doi:10.5194/acp-16-13379-2016, 2016.
- Weiss-Penzias, P., Amos, H. M., Selin, N. E., Gustin, M. S., Jaffe, D. A., Obrist, D., Sheu, G. R. and Giang, A.: Use of a global model to understand speciated atmospheric mercury observations at five high-elevation sites, *Atmos. Chem. Phys.*, 15(3), 1161– 1173, doi:10.5194/acp-15-1161-2015, 2015.

